STABILITY CONTROL OF A 6 DOF BIPED IN THE DUAL-SUPPORT PHASE USING FUZZY CONTROL

CEDRIC COCAUD
Department of Mechanical Engineering, University of Ottawa, 770 King Edward Ave.
Ottawa, Ontario K1N 6N5, Canada,

AMOR JNIFENE
Department of Mechanical Engineeringy, University of Ottawa, 770 King Edward Ave.
Ottawa, Ontario K1N 6N5, Canada,
jnifene@eng.uottawa.ca

Abstract

This work investigates the feasibility of using a fuzzy controller to stabilize a biped robot in the dual-support phase. Taking as inputs the errors of the angular position and angular velocity for each joint, the controller uses a rule-base implemented with five membership functions to compute the joint torques of a 6 DOF biped robot. The input gains were computed at run-time using the Hip and Ankle Strategy (HAS), which sets a gain value for each joint based on the relative position of the center of gravity with respect to the support area. Although the Hip and Ankle Strategy was found to increase the computational load without enhancing the actuation response, the results have clearly showed the success of the fuzzy control scheme in making the non-linear system stable, as well as in placing the robot into the most stable posture without having to lift the feet of the ground.

1. Introduction

Biped robots have been an emerging interest in the field of robotic. Their method of locomotion would make them far more versatile than conventional wheeled robots when considering the greater number of terrains over which they could operate without difficulties. In parallel with research aiming to enhance the robot decision-making abilities based on increasingly advanced intelligent software, there is a need to develop low-level control software that deals with the mechanics of the robot. Due to the highly non-linear dynamics of robotic systems, many approaches have been studied. Starting with the classical computed torque method [1] which attempts to linearize the system by integrating a model of the non-linear terms in the controller. The tendency of control system designers has evolved progressively toward more robust control schemes. Unfortunately, biped robots present the added difficulty of not having a fixed base resulting in stability problems at all stages of the walking cycle. Moreover, a true reproduction of human legs configuration results in an over actuated system for which standard control methods are not adequate. Many papers have dealt with these problems by using a broad range of simplifications such as constraining the motion within the sagittal plane (reducing the problem to 2-D and reducing the number of DOF to a minimum) [2,3], using the inverted pendulum approximation for the sagittal and/or the lateral plane [4], and omitting the dual support phase (assuming that the support feet exchange is instantaneous) [5]. The great majority of the studies done on modeling bipeds have used the Lagrange method, accounting for the holonomic constraints by means of the Lagrange multipliers [6,7,8].

Control schemes for biped robots have varied from the simplest feedforward compensation and linear state feedback [8] to computed torque methods and impedance control [6,9], the latter case being essentially a hybrid force and position control. Another approach was the sliding-mode control presented in [5], which consists of defining a vector field (in velocity state-space) pointing toward the desired trajectory that each link must follow. A control law based on the second method of Lyapunov and on sliding mode is derived in order to establish a stable controller that forces all links to converge to the ideal trajectories. As it can be found in many works on biped control, the impact force is usually considered as a measurable variable. Due to the difficulty in measuring this force accurately, these control schemes may prove to be difficult to implement.

In general, the control schemes developed for bipeds are based on following a predefined trajectory, which must be changed depending on the type of action undertaken (running, walking, climbing stairs, etc.) and the type of ground relief considered. Moreover, these trajectories must take into account both the balance of the system as it moves, and the motion itself. A number of researches have worked to circumvent these difficulties by dealing with stability and motion separately. As such, the concept of a Central Pattern Generator consisting of a set of neurons able to produce rhythmic motion patterns without the need for sensory feedback, emerged with the complementary Reflex module that rely heavily on sensor-motor-feedback to maintain balance [10,11]. Other high-level control schemes were elaborated such as the "Hip and Ankle Strategy" (HAS), which is based on the suggestion that the Central Nervous System simplifies complex motor actions by fixing from prior experiences the interaction among a group of muscles. Starting from this concept, the authors of [12] developed a pseudo-code that implements this control scheme using a set of if-then-else rules. This approach diverged from more conventional ones that optimized energy cost functions to find the best effort distribution among all actuators (be it motors or muscles).

Aiming to combine our intuitive knowledge of walking, with the concept of having separate modules that deals independently with stability and motion, the present paper proposes a control scheme based on fuzzy logic [13]. The dual-support phase of a biped robot was selected in order to investigate the potential of fuzzy logic in solving the over actuation problem without having to optimize some energy cost function in the process. The objectives of the research presented in this paper are to establish and test a control scheme that is not based on a trajectory following approach, while avoiding at the same time the integration of complex models into the controller.

2. Dynamics of the 6-DOF Biped System

Figure 1 shows the 6 DOF biped robot used in the analysis. The orientation and position of the frames at each joint are determined based on the Denavitt Hartenburg convention commonly used in the analysis of serial kinematic chains. The reference frame for the overall system is taken as $X_{0g}Y_{0g}Z_{0g}$ located at the foot of the support leg. The non-support leg will be referred as the free leg. The stability of the biped will be analyzed when the free leg is at various positions with respect to the support leg. The variables q_1 to q_6 represent the joint angles and a_1 and a_2 are the lengths of the lower and upper parts of the leg, respectively. L_R and L_F are two dimensions representing the length of the foot. A concentrated mass is assumed at each of the six joints and the center of mass of the entire biped is assumed to be at point G.

During the transition phase of the walking cycle, the dynamics of a biped robot can be treated as a open kinematic chain with one foot as the base and the other foot as the free end. During the dual-support phase, where both feet are on the ground, the dynamics of the biped is subject to holonomic constraints if we assume that the contact points between the ground and feet are fixed within the reference frame. These constraints can be described in the dynamic model by using the Lagrange multiplier λ_j as follows:

$$\frac{d}{dt}\left(\frac{\partial L}{\partial \dot{q}_i}\right)-\frac{\partial L}{\partial q_i}=T_i-\sum_{j=1}^{j=m}\lambda_j\frac{\partial\, c}{\partial q_i} \qquad (1)$$

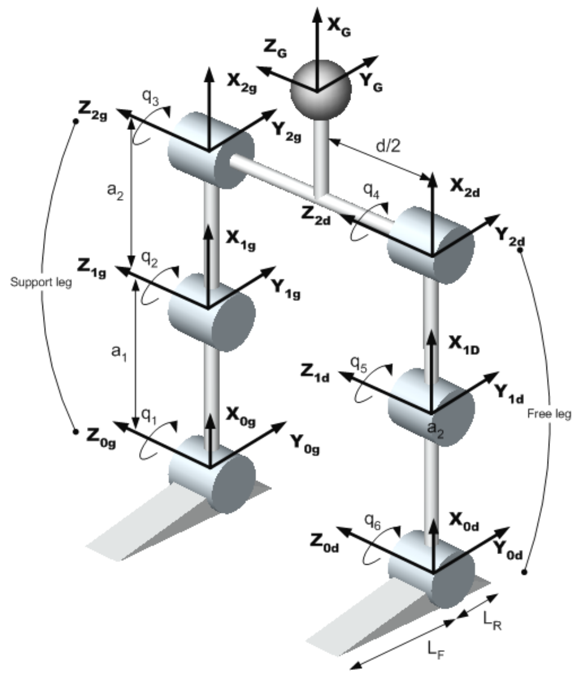

Figure 1: Reference frames of the biped robot using DH convention

where L is the Lagrangian of the system $L=K-U$, K is the kinetic energy of the system and U is the potential energy, q_i is the generalized coordinate of joint i, T_i is the input torque at joint i, and $c(q)$ is the mathematical relation that defines the geometrical constraints. Figure 2 shows the relations between the joint angles when the biped is in the dual support mode.

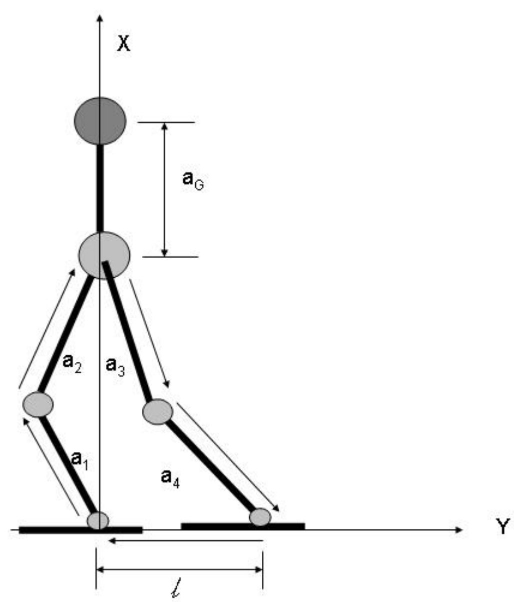

Figure 2: Biped robot in the dual support phase

Assuming that $a_1 = a_4$ and $a_2 = a_3$, the x and y components of the vector linking the first frame (i.e. left foot) to the last frame (i.e. right foot) must satisfy the following conditions

$$\begin{aligned} & a_1(\cos(q_1) - \cos(q_1 + q_2 + q_3 + q_4 + q_5)) \\ & + a_2(\cos(q_1 + q_2) - \cos(q_1 + q_2 + q_3 + q_4)) = 0 \end{aligned} \tag{2}$$

and

$$\begin{aligned} & a_1(\sin(q_1) - \sin(q_1 + q_2 + q_3 + q_4 + q_5)) \\ & + a_2(\sin(q_1 + q_2) - \sin(q_1 + q_2 + q_3 + q_4)) = l \end{aligned} \tag{3}$$

re-arranging the above two equations and denoting by $c_i = \cos(q_i)$, $s_i = \sin(q_i)$, $c_{ij} = \cos(q_i + q_j)$, and $s_{ij} = \sin(q_i + q_j)$, the geometric constrains can be written in matrix form as

$$c(q) = \begin{bmatrix} a_1 \left(c_1 - c_{12345}\right) + a_2 \left(c_{12} - c_{1234}\right) \\ a_1 \left(s_1 - s_{12345}\right) + a_2 \left(s_{12} - s_{1234}\right) - l \end{bmatrix} = \begin{bmatrix} 0 \\ 0 \end{bmatrix} \tag{4}$$

Denoting by C the 2x6 matrix defined by $C = \frac{\partial c(q)}{\partial q} = \begin{bmatrix} \frac{\partial c(q)}{\partial q_1} & \frac{\partial c(q)}{\partial q_n} \end{bmatrix}$, and after evaluating the Lagrangian of the biped robot, the joint accelerations can be obtained from Equation 1 and written as

$$\ddot{q} = M^{-1}\left(\tau - C^T \lambda - N(q, \dot{q}) - P(q)\right) \tag{5}$$

The $C^T\lambda$ terms correspond to the joint torques caused by the reaction forces between the feet and the ground. $N(q, \dot{q})$ is a 6x1 vector representing the coriolis and centrifugal terms, $P(q)$ is a 6x1 vector representing the gravity terms, and τ is a 6x1 vector representing the input torque at the joints. Differentiating Equation 4 twice with respect to time gives

$$\dot{C}\, \dot{q} + C\, \ddot{q} = 0\,. \tag{6}$$

Substituting Equation 5 into Equation 6 and solving for the Lagrange multipliers λ give

$$\lambda = \left(C M^{-1} C^T\right)^{-1} \left[C M^{-1} \left(\tau - N(q, \dot{q}) - P(q)\right) + \dot{C}\, \dot{q}\right] \tag{7}$$

The complete dynamics of the biped robot in the dual support can be described by the two equations (5) and (7).

3. Biped Stability Control

This section is to assess the performance of a controller based on fuzzy logic to stabilize a biped robot in the dual-support phase. In this phase, the system becomes over actuated which leads to multiple solutions. The goal is to stabilize the robot by forcing it to adopt a predefined optimal balanced posture. The joint velocities and joint angular positions are used as inputs to the proposed fuzzy controller. This choice is motivated by the fact that fuzzy controllers based on position and velocity feedback have already been successfully used to control the stability of single and multi-link inverted pendulums. The obvious similarity between these systems and a biped robot system suggest that the latter could be effectively controlled using the same strategy. In a general trajectory planning control scheme, this type of controller would follow a trajectory characterized by a series of pre-defined joint-space variables. In the particular problem of walking bipeds, failing to follow such trajectories (by being either too slow or to fast) can result into dynamic instabilities and eventually, complete failure in achieving the goal task (i.e. the robot is unable to resume its walking cycle). In this case, no predefined trajectory is specified. Each joint is controlled independently based on its specific position and velocity errors. All joint motions are managed according to the same control rules. The position error and the velocity error are defined as the difference between the actual angular position and angular velocities and the ones specified by the desired posture (i.e. the joint variables describing the pre-defined optimal balanced posture). The goal of the controller is to minimize the error, and ideally, to reduce it to zero. However, it will be seen later on that the error does not need to be zero in order to reach the optimum balanced position.

3.1 ***Controller overview***

The scope of this work is limited to the biped stability control for the dual-support phase. Therefore, it does not include reaching stability by modifying the support area (i.e. moving a foot in some direction to make the body center of gravity fall into an extended stable area). Since it is not possible to recover from a point where the center of gravity is beyond the support area without extending this area by moving one or both feet, the starting position of the center of gravity will have to be restricted to a position between the extremities of both feet. External forces and moments concentrated on the body center of gravity are used as external disturbances to simulate the biped stability. Moreover, it is assumed that these forces can be contained within the sagittal plane.

3.1.1 *Controller structure*

The controller is composed of two parts. The first one corresponds to a high-level fuzzy controller that evaluates the current robot configuration in terms of the position of its center of gravity within the support area. The second part is a low level fuzzy controller that takes care of evaluating the output torques of the six joints based on the desired position and velocity of each joint. Since we want to achieve static stability, the desired velocity will always be zero for all joints. The high-level controller (HLC) determines the strategy to apply in a given situation. Depending on the configuration of the robot (i.e. how close is body's center of gravity from the limits of the support area), the controller can either give more weight to the hip joints or the ankle joints. In the eventuality that the robot is in a stable position, the controller may divide the actuation effort equally between all joints. This strategy is inspired by the work of [12]. The main function of the HLC is to select the input gains for the low-level controller. These gains increase the magnitude of the error for a selected sub-group of joints. The low-level controller (LLC) is the actual controller that computes the torques required at each joint. The same sets of fuzzy rules and membership functions are used for each joint. As mentioned earlier, these rules determine the actuation torque based on the magnitude of the error of the angular velocity and position. Figure 3 shows an overall structure of the control system.

3.1.2 *High-level fuzzy controller*

The HLC has as input variables the angular position of the 6 joints and as output a vector of 6 elements containing the input gain for each joint. The input membership functions are shown in Figure 4.

The universe of discourse defined by the negative and positive boundaries is defined based on the distance from the reference frame at the support foot, and the tip of the free foot. Depending on the relative position of the free foot with respect to the support foot, three cases are possible as described in Figure 5. Taking the position of the center of gravity along the horizontal axis (with the support foot as the reference frame), it is possible to calculate the certainty of each membership function. From there, the following sets of rules apply to determine the gain vector K for the input of the LLC.

if (strategy = zero) then K = [1, 1, 1, 1, 1, 1]
if (strategy = Ankle) then K = [μ, 1, 1, 1, 1, μ]
if (strategy = Hip) then K = [1, 1, μ, μ, 1, 1]

with μ > 1.

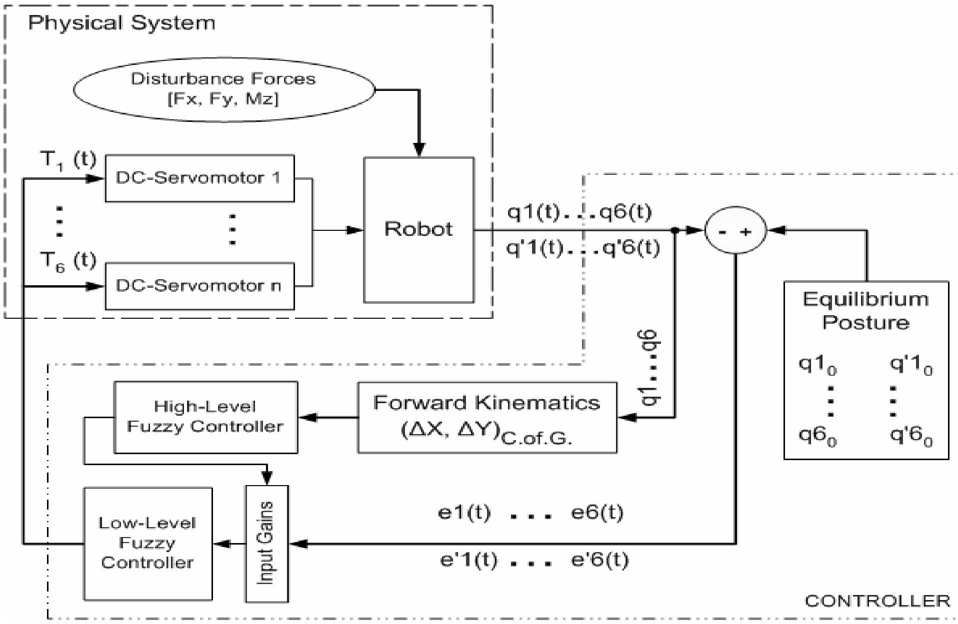

Figure 3: Controller overview

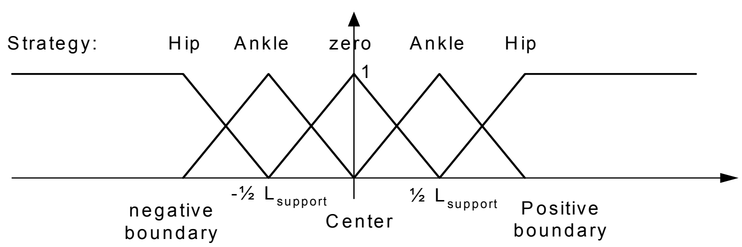

Figure 4: HLC input membership function

The certainty of the three premises shown above will be labelled P_{zero}, P_{ankle} and P_{hip}. Since the fuzzification process will result in a maximum of two active membership functions (and a minimum of one), at least one of the P_x values will be zero. However, its value will still be needed in the defuzzification process. This process is performed using the following equation for each joint:

$$K_i = P_{zero}K_{zero,i} + P_{ankle}K_{ankle,i} + P_{hip}K_{hip,i} \qquad i = 1,2,\ldots 6, \qquad (8)$$

and $K_{zero,\,1\ldots6}$ = [1, 1, 1, 1, 1, 1], $K_{ankle\,1\ldots6}$ = [μ, 1, 1, 1, 1, μ], $K_{hip\,1\ldots6}$ = [1, 1, μ, μ, 1, 1].

Based on Equation (8) it can be seen that the input gain of the knees will always be 1, while the hip and ankle input gains will vary between 1 and μ depending on the fuzzy sets defining the position of the center of gravity.

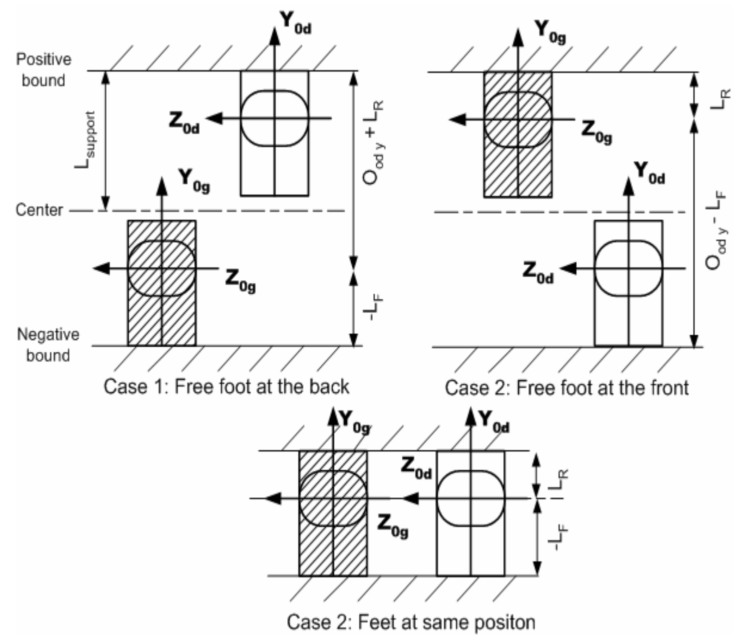

Figure 5: Feet configurations

3.1.3 *Low-level fuzzy controller*

The low-level controller (LLC) determines the torques required at each joint to maintain or increase the stability of the system. The problem being very similar to the inverted pendulum [13], the same input variables are used (i.e. angular positions and velocities) and the same fuzzy rules are implemented here. A summary of these rules is shown in Table 1. The labels –L, -S, +S and +L stands for negative large, negative small, positive small and positive large respectively. It is assumed that the angular position of each joint varies between $-\pi/2$ and $\pi/2$ and the angular velocity varies between $-\pi/4$ rad/sec and $\pi/4$ rad/sec. The output is limited by the size of the actuator at each joint and can vary between $-T_{\max}$ and $T_{\max}$. Figures 6 and 7 show the inputs and the output membership functions of the low level joint controller, respectively.

Table 1: Summary of LLC fuzzy rules

Torque (N m)			Angular Position Error (rad)				
			-L	*-S*	*0*	*+S*	*+L*
			- π / 2	*- π / 4*	*0*	*π / 4*	*π / 2*
Angular Velocity Error (rad /s)	*-L*	*- π / 4*	- T_{max}	- T_{max}	- T_{max}	-½ T_{max}	0
	-S	*- π / 8*	- T_{max}	- T_{max}	-½ T_{max}	0	½ T_{max}
	0	*0*	- T_{max}	-½ T_{max}	0	½ T_{max}	T_{max}
	+S	*π / 8*	-½ T_{max}	0	½ T_{max}	T_{max}	T_{max}
	+L	*π / 4*	0	½ T_{max}	T_{max}	T_{max}	T_{max}

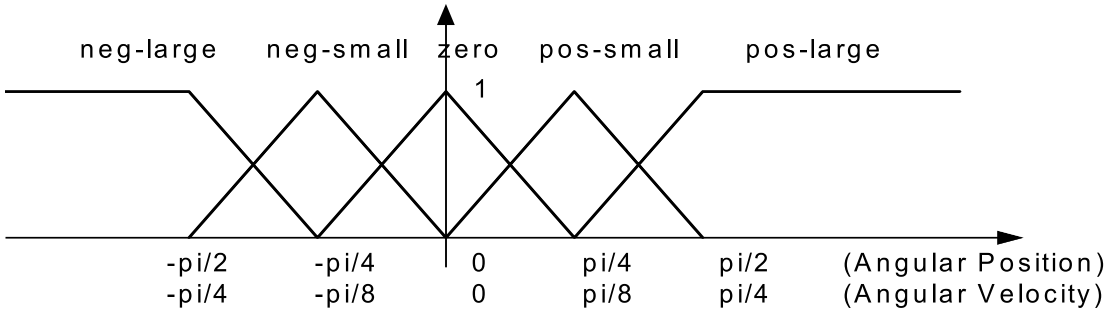

Figure 6: LLC input membership functions

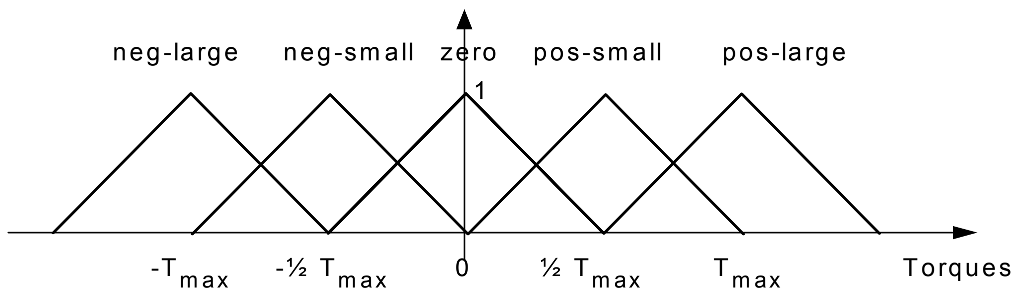

Figure 7: LLC output membership functions

It is important to emphasize the fact that the two universes of discourse represented in Figure 6 actually correspond to the position and velocity errors associated with each joint, multiplied by the input gain computed by the HLC. So the input for the LLC is of the form:

Angular position:

$$e = [e(q_1)K_1, \quad e(q_2)K_2, \quad e(q_3)K_3, \quad e(q_4)K_4, \quad e(q_5)K_5, \quad e(q_6)K_6\ ] \qquad (9)$$

Angular velocity:

$$\dot{e} = [\dot{e}(q_1)K_1, \quad \dot{e}(q_2)K_2, \quad \dot{e}(q_3)K_3, \quad \dot{e}(q_4)K_4, \quad \dot{e}(q_5)K_5, \quad \dot{e}(q_6)K_6\ ] \qquad (10)$$

with $\dot{e}(q_i)$ the angular velocity error associated with joint *i*. The "minimum" operator is used to evaluate the certainty of the premises when two membership functions are activated for a given variable and the output is calculated using the COG (Center of gravity) method.

4. Simulation of the 6-DOF Biped

Simulations were conducted using Matlab/Simulink. These simulations are to analyze the performance of the fuzzy controller in stabilizing the biped robot described by the dynamic model derived in section 2. Studies in biomechanics have shown that the mass distribution of a human body gives a ratio of 19% of the total body mass for each leg, and 62% for the upper-part of the body. Based on this distribution, the mass and the size of each of the legs and of the upper part of the biped were selected. The masses of the legs are assumed to be concentrated at the joints and the mass of the upper part is assumed to be concentrated at point G. The length of each link and location of the center G with respect to the hip joint are taken based on the proportions of the human body. Table 2 shows the proportions of the biped used in this simulation.

Table 2: Biped characteristics

Parameter	Value
a_G	0.15 *m*
a_2=a_3	0.225 *m*
a_1=a_4	0.225 *m*
d	0.26315 *m*
L_R	0.05625 *m*
L_F	0.1125 *m*
T_{max}	1.24 *N·m*

In order to test the performance of the 6 DOF biped under the proposed fuzzy control, the ability of the biped to return to a pre-defined posture (reference position) starting from an initial posture is examined. The initial posture is defined by an initial joint angle for each of the six joints describing the motion of the biped. This test will show if the biped can recover from a loss of balance without having to move the feet off the ground. The initial posture used in the simulation is shown in Figure 8 and the corresponding joint angles are given in Table 3.

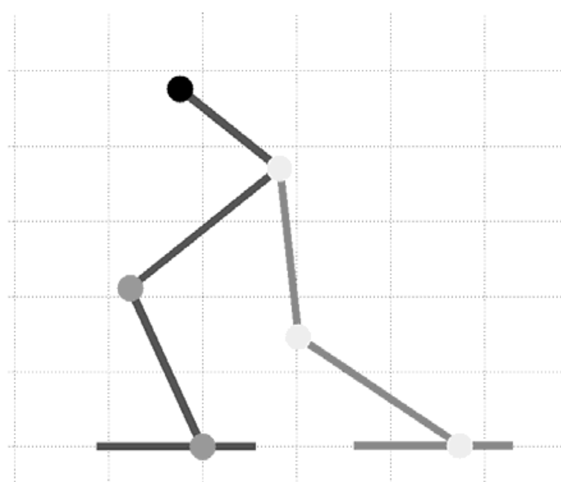

Figure 8: Initial posture

Table 3: Initial angular positions

Support leg			*Free leg*		
Ankle	Knee	Hip	Hip	Knee	Ankle
-20	65	-90	40	-45	50

The desired equilibrium position is defined by the joint angles shown in Table 4

Table 4: Desired posture

Support leg			*Free leg*		
Ankle	Knee	Hip	Hip	Knee	Ankle
β	0	- β	- β	0	β

Where $\beta = \pi / 2 - \text{acos}((l/2)/(a1+a2))$ and l is the distance between the two ankles.

Preliminary results showing the performance of the control scheme presented in this paper are shown in Figure 9 and Figure 10. The time response of q_3 and q_4 during the recovery from a loss of balance as shown in Figure 9.a indicates that the upper body has the slowest response. Starting from a posture where the body is bent forward, the hips gradually move to the center of the support area without altering much the inclination of the trunk. Once all the links are closer to their desired positions (at $t \approx 0.25$ secs.) the hip joints gradually rotate the trunk to its desired position. Based on the Hip and Ankle Strategy, the initial posture should fall into the Hip Strategy area and therefore puts more weight on the error of the hip joints such that the system first rotates the trunk up to the vertical axis. However, the error signals of the knee joints result in a large torque response which brings point G to the Ankle Strategy area very quickly (within 0.25 sec).

Figure 10 shows the contribution of each of the Hip and Ankle strategies during the recovery phase as calculated by the high level fuzzy controller. The figure shows that the recovery starts with 20% of the control effort is due to the hip joints and 80% is due to the ankle joints. As the biped is near the desired posture, the control effort is split based on the ankle strategy and the zero strategy. At t=1.2 sec, the biped passes by the desired position and at this instant 100% of the control effort is based on the zero strategy. Since stabilizing a biped in the double support phase is similar to the problem of stabilizing an inverted pendulum, the desired position is in fact open-loop unstable and to in order to stabilize the system at this position, the fuzzy controller splits the control effort between the zero strategy and the ankle strategy as shown in Figure 10 when $t > 1.2$ sec.

In order to assess the impact of the *Hip and Ankle Strategy*, the effect of increasing the multiplier μ will be investigated and further discussion will be included in the final version of the manuscript. As described in section 3.1.2, this multiplier essentially plays the role of a varying input gains vector for the error on the angular velocities and positions. Depending on the robot posture, the Hip and Ankle Strategy (HAS) puts more weights on the hip or ankle joints according to the employed strategy. As it was implemented, this high-level fuzzy controller only takes into account the position of the center of gravity with respect to the support area. It does not take in account the particular configuration of the legs. Further studies could include an implementation of the Hip and Ankle Strategy taking into account the legs configuration rather than just the center of gravity. It may then be possible to increase the actuation force where it is truly necessary without excessive energy expenditure.

5. Conclusion

The goal of this work was to assess the feasibility of using fuzzy logic to stabilize a biped during the dual-support phase. Taking as inputs the angular position and the angular velocity for each joint, the controller used a rule-base implemented with five membership functions to control the output torques. The input gains were computed at run-time using the Hip and Ankle Strategy, which sets a gain value for each joint based on the relative position of the center of gravity with respect to the support area. The results have clearly showed the success of the fuzzy control scheme in stabilizing a highly non-linear system such as the one describing the dynamics of a biped robot. The proposed fuzzy control was used to allow the biped robot recover from a loss of balance defined by a pre-defined initial posture. Simulations using the *Hip and Ankle Strategy* showed this control scheme only increased the computational load along with the actuation load imposed on the motors. The same conclusions were drawn from simulations aiming to enhance the system performances by increasing the number of membership functions. The dynamic model used in this paper showed some deficiencies when testing parallel legs configurations. These configurations lead to a singularity in the over all mass matrix. A dynamic model that takes into account the length and the mass of each foot would be more realistic. Also, adding a joint in the middle of the foot (representing the junction at the toes) could solve the singularity problem of the mass matrix by making it impossible to align all joints along the same line. Finally, fuzzy control seems to be a promising approach to control bipeds due to its simplicity and robustness and will be extended to cover the full walking cycle of the biped.

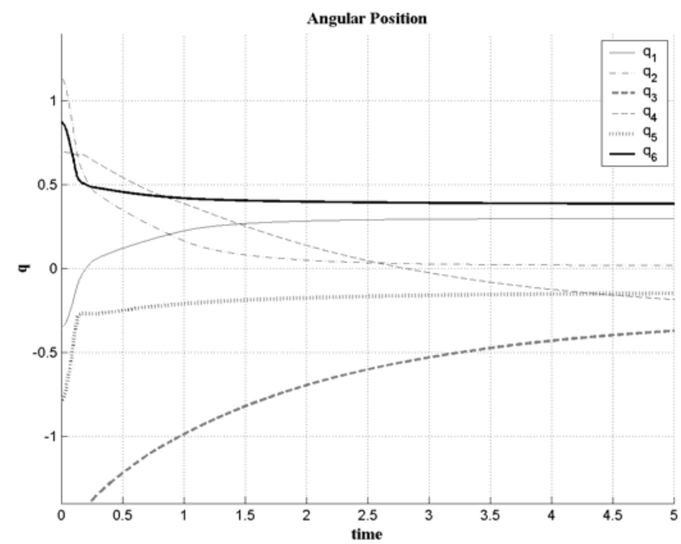

(a)

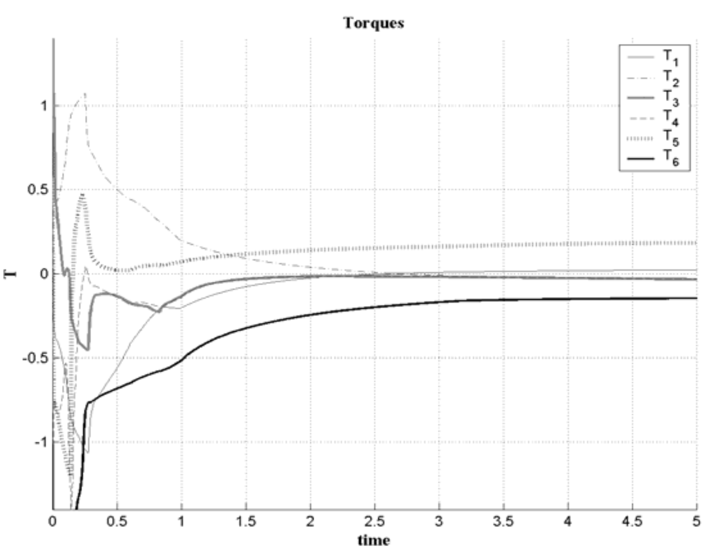

(b)

Figure 9: a) Angular positions during the recovery (rad). b) Applied torques during the recovery (N.m). (μ=2).

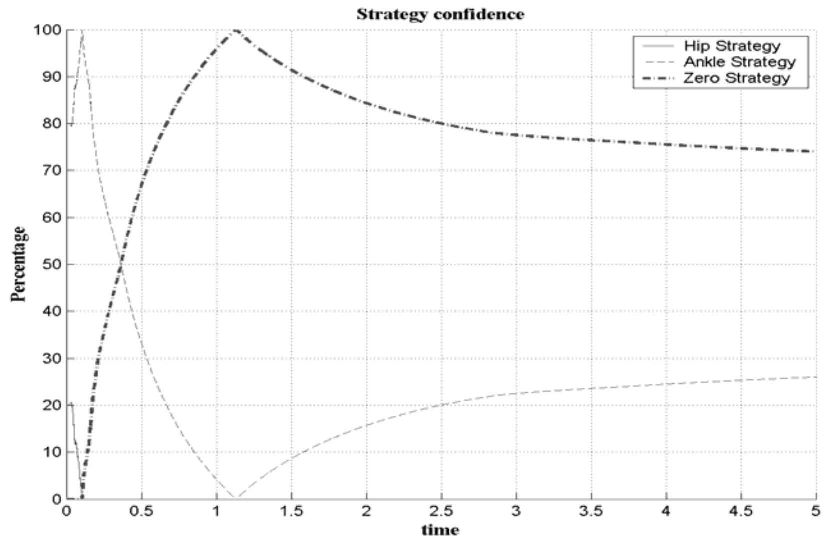

Figure 10: Strategies employed during the recovery (μ=2)

6. References

1. H. K. Lum, M. Zribi, Y.C. Soh, Planning and control of a biped robot, *International Journal of Engineering Science*, 37, pp 1319-1349 (1999).

2. K. Ono, R. Liu, Optimal biped walking locomotion solved by trajectory planning method, *Journal of Dynamic Systems, Measurements, and Control*, *Transaction of the ASME*, **124**, pp 554–565 (2002).

3. K. Mitobe, N. Mori and Y. Nasu, Control of a biped walking robot during the double support phase, *Autonomous Robots*, **4**, pp 287-296 (1997).

4. K. Majima, T. Miyazaki, K. Ohishi, Dynamic gait control of biped robot based on kinematics and motion description in Cartesian space, *Electrical Engineering in Japan*, **129** (4), pp 96-104 (1999).

5. S. G. Tzafestas and T. E. Krikochoritis, Robust sliding-mode Control of Nine-link Biped Robot Walking, *Journal of Intelligent and Robotic Systems*, **20**, pp 375-402 (1997)

6. Jong Hyeon Park and Hoam Chung, Hybrid control of biped robots to increase stability in locomotion, *Journal of Robotic Systems*, **17** (4), pp 187-197 (2000)

7. S. Caux and R. Zapata, Modeling and control of biped robot dynamics, *Robotica*, **17**, pp 413-426 (1999)

8. Ching-Long Shih and William A. Gruver, Control of a biped robot in the double-support phase, *IEEE transactions on systems, man, and cybernetics*, **22** (4), pp 729-735 (1992)

9. P. Gorce and M. Guihard, On dynamic control of pneumatic bipeds, *Journal of Robotic Systems*, **15** (7), pp 421-433 (1998)

10. B. Klaassen, R. Linnemann, D. Spenneberg, F. Kirchner, Biologically inspired robot design and modeling, in *ICAR 2003, 11th Int. Conf. Advanced Robotics*, (IEEE Press, Coimbra, Portugal, 2003), pp 576-581

11. Zhang Xiuli, Zheng Haojun, Duan Guanghong, Wang Jinsong, CPG-based Bio-gait research of the quadrupedal robot, in *ICAR 2003, 11th Int. Conf. Advanced Robotics*, (IEEE Press, Coimbra, Portugal, 2003), pp 1009-1013

12. M. Guihard and P. Gorce, Biologically inspired behaviour: hip strategy applied to humanoid robot, in *ICAR 2003, 11th Int. Conf. Advanced Robotics*, (IEEE Press, Coimbra, Portugal, 2003), pp 1393-1398

13. K. M. Passino and S. Yurkovich, *Fuzzy Control*, (Addison Wesley, 1998), Chapter 2.